NACA TN No. 1780

8227

TECH LIBRARY KAFB, NM
0065007

NATIONAL ADVISORY COMMITTEE FOR AERONAUTICS

TECHNICAL NOTE

No. 1780

CHARTS FOR THE CONICAL PART OF THE DOWNWASH FIELD OF SWEPT WINGS AT SUPERSONIC SPEEDS

By Jack N. Nielsen and Edward W. Perkins

Ames Aeronautical Laboratory
Moffett Field, Calif.

Washington
December 1948

TECH LIBRARY KAFB, NM

0065007

NATIONAL ADVISORY COMMITTEE FOR AERONAUTI

TECHNICAL NOTE No. 1780

CHARTS FOR THE CONICAL PART OF THE DOWNWASH FIELD OF SWEPT WINGS AT SUPERSONIC SPEEDS

By Jack N. Nielsen and Edward W. Perkins

SUMMARY

Analytical expressions have been derived for the downwash throughout the entire induced flow field of lifting triangles of infinite chord with leading edges either in front of or behind the Mach cone. These expressions have been determined from the line-pressure source theory of R. T. Jones and the lifting-triangle investigation of H. J. Stewart. Based on these analytical results, downwash charts have been prepared from which the downwash field may be determined for any practical combination of leading-edge sweep angle and flight Mach number. These charts for the lifting triangle of infinite chord are basic to the solution for the downwash field of any finite swept wing wherein the contributions of the tips and the trailing edges are to be determined by the method of lift cancellation as employed by Lagerstrom and others. The conical part of the downwash is obtained from the charts, and the nonconical part must be obtained by other means such as the lift-cancellation method.

INTRODUCTION

One of the principal requirements for a rational analysis of the longitudinal stability of aircraft is a knowledge of the downwash field behind lifting surfaces. Theoretical methods based on lifting-line theory for determining downwash for conventional lifting surfaces at subsonic speeds are well known. However, before satisfactory agreement between experiment and theory was obtained, the theoretical downwash had to be corrected for the local effects of the wake and the vertical displacement of the trailing vortex sheet (e.g., reference 1). The methods of reference 1 are applicable to conventional airplanes throughout the subcritical speed range by use of the Glauert-Prandtl rule (reference 2). No practical method exists at present for the calculation of downwash in the supercritical speed range.

Several methods based on solutions of the linearized differential equation of compressible flow are available for determining the theoretical downwash at supersonic speeds. By the use of the conical flow theory of Busemann (reference 3), Lagerstrom in reference 4 has developed analytical expressions for the downwash field of certain uniformly loaded lifting surfaces. By superposition of these lifting surfaces, Lagerstrom has determined the downwash field of a flat rectangular wing and a flat trapezoidal wing. In addition he has indicated a method for determining the effect on the downwash field of adding a trailing edge to a lifting triangle of infinite chord to form a finite wing. Heaslet and Lomax (reference 5) have determined the downwash for points along the intersection of the chord plane with the vertical plane of symmetry behind a finite triangular wing with subsonic leading edges. They have also determined an approximate solution for the downwash in the vicinity of this line at an infinite distance behind the wing. The Schlicting vortex theory can be used to calculate the downwash induced by various span load distributions. The concepts employed are analogous to the Prandtl lifting-line theory and as such consider only the spanwise lift distribution and hence neglect any possible effects of chordwise lift distribution.

No determination has been made of the downwash throughout the induced flow field of a swept wing in supersonic flow. The solution for the downwash field for a lifting triangle of infinite chord is basic to the solution for the downwash field of any finite swept wing wherein the contribution of the tips and the trailing edge are to be determined by the method of lift cancellation as employed by Lagerstrom in reference 4. For a finite swept wing, the conical downwash field of the lifting triangle of infinite chord represents the entire downwash field except for the regions of influence of the tips and trailing edge. Within these regions, it represents an appreciable contribution to the downwash.

The purpose of the present investigation was to determine analytical expressions for the downwash throughout the entire induced flow field for flat lifting triangles of infinite chord with either subsonic or supersonic leading edges. These expressions are used in the construction of nondimensional downwash charts, which, when used in conjunction with the lift-cancellation method, provide a practical means of determining the downwash field for finite swept wings. Although the analysis was carried out for $M_o^2 = 2$, the charts are presented in a form making them applicable to any supersonic Mach number. The charts are subject to the usual limitations of linear theory.

SYMBOLS

Primary Symbols

α	angle of attack
r.p.	real part of a complex function
V_o	free-stream velocity
M_o	free-stream Mach number
m	cotangent of the sweep angle of the wing leading edge
$\left\lvert\frac{dz}{dx}\right\rvert$	slope of the surface of the wedge section in the streamwise direction
x,y,z	longitudinal, lateral, and normal coordinates with the origin at the apex and the $z = 0$ plane coincident with the chord plane of the wing. (The positive directions are indicated in fig. 1.)
x',y',z'	oblique coordinates, $x' = x-my$, $y' = y-mx$, $z' = z\sqrt{1-m^2}$
φ	potential of the perturbation velocities
u,v,w	perturbation velocities in x-, y-, and z-directions, respectively
W	downwash function $(w + i\overline{w})$
$\overline{w}$	harmonic conjugate of w
ζ	complex variable $(se^{i\theta})$
s	$\dfrac{\sqrt{(y/x)^2+(z/x)^2}}{1+\sqrt{1-(y/x)^2-(z/x)^2}}$
θ	$\tan^{-1}\left[\dfrac{(y/x)}{(z/x)}\right]$
s_o	$\sqrt{\dfrac{1-\sqrt{1-m^2}}{1+\sqrt{1-m^2}}}$
ϵ	downwash angle $(-w/V_o)$

$E(\sqrt{1-m^2})$ complete elliptic integral of the second kind with modulus $\sqrt{1-m^2}$

ξ,η complex variables

$F(\xi,\sqrt{1-s_o^4})$ incomplete elliptic integral of the first kind with modulus $\sqrt{1-s_o^4}$ and sine amplitude ξ

$$\left[\int_0^{\xi}\frac{d\xi}{\sqrt{1-\xi^2}\sqrt{1-(1-s_o^4)\xi^2}}\right]$$

$E(\xi,\sqrt{1-s_o^4})$ incomplete elliptic integral of the second kind with modulus $\sqrt{1-s_o^4}$ and sine amplitude ξ

$$\left[\int_0^{\xi}\frac{\sqrt{1-(1-s_o^4)\xi^2}}{\sqrt{1-\xi^2}}\,d\xi\right]$$

C constant of integration

τ real part of a complex variable

δ imaginary part of a complex variable

F_r real part of the incomplete elliptic integral of the first kind

F_i imaginary part of the incomplete elliptic integral of the first kind

E_r real part of the incomplete elliptic integral of the second kind

E_i imaginary part of the incomplete elliptic integral of the second kind

k modulus of elliptic integrals $(\sqrt{1-s_o^4})$

k' comodulus of elliptic integrals $(\sqrt{1-k^2})$

sn Jacobian sine amplitude elliptic function

cn Jacobian cosine amplitude elliptic function

dn	Jacobian delta amplitude elliptic function
$\sqrt{\lambda}$	$sn(F_r,k)$
$\sqrt{\sigma}$	$sn(F_i,k')$
μ	incomplete elliptic integral of first kind of sine amplitude ξ and modulus k

Subscripts

P	value at point P
Q	value at point Q
c	value at Mach cone
wc	value between plane wave and Mach cone
1	refers to complex variable ξ
2	refers to complex variable η
r	refers to real part of a complex variable
i	refers to imaginary part of a complex variable

LIFTING TRIANGLE OF INFINITE CHORD WITH SUPERSONIC LEADING EDGES

In the theory of supersonic conical flow, the downwash field of a flat lifting triangle is symmetrical about both the chord plane and the vertical plane of symmetry. The downwash field above or below the flat lifting triangle at angle of attack α is the same as the downwash field below a nonlifting triangular wing of the same plan form with a streamwise wedge-shaped section of half angle α, since the flows above and below the wings are independent. (See fig. 1.) The downwash field for this nonlifting triangular wing may be determined from its streamwise perturbation velocity field which may be obtained from the results presented by R. T. Jones in reference 6. The streamwise perturbation velocity field, or the u-field, for the nonlifting triangular wing is the sum of the u-fields for two line pressure sources coincident with its leading edges. Similarly, the downwash field for the wing is the sum of the downwash fields for the two line pressure sources. However, since the downwash field for one line

source is the reflection in the xz-plane of the downwash field for the other line source, it is sufficient to determine an expression for the downwash of a single line source. The complete downwash field is then determined as the sum of the field given by this expression and the field given by this same expression with the sign of the lateral dimension reversed.

R. T. Jones in reference 6 gives the following equation for the perturbation velocity u at any given point in the field for a line pressure source in front of the Mach cone.

$$u = -\,\mathrm{r.p.}\ \frac{V_0}{\pi}\frac{m}{\sqrt{m^2-1}}\left|\frac{dz}{dx}\right| \cos^{-1}\left(\frac{x'}{\sqrt{y'^2+z'^2}}\right) \tag{1}$$

In this equation $|dz/dx|$ is equal to α as previously discussed. It should also be pointed out that the positive root of the radical $\sqrt{y'^2 + z'^2}$ should be used in conjunction with the principal value of the inverse cosine. In the succeeding analysis, the downwash field for the upper surface of the nonlifting wing will be determined. However, since the downwash field for this wing is antisymmetric about the chord plane, it will be necessary to reverse the sign of the result for application to the upper surface of the lifting triangle.

The perturbation potential φ at any point P may be evaluated as the line integral of u along the line parallel to the x-axis through the point P.

$$\varphi = \int_{x_l}^{x} u\,dx \tag{2}$$

for which the lower limit x_l corresponds to a point outside the region of influence of the line source where the values of φ and u are zero. The region of influence of the line source is bounded by the Mach cone and the plane waves from the line source tangent to the Mach cone. (See fig. 1.) Figure 2 shows two possible paths of integration for equation (2). The path corresponding to point P of this figure intersects only the Mach cone; whereas the path corresponding to point Q intersects both the plane wave $(y'^2+z'^2 = 0)$ and the Mach cone $(x^2 = y^2+z^2)$. Consider first point P: The perturbation potential is given by

$$\varphi_P = \int_{\sqrt{y^2+z^2}}^{x} u\,dx \tag{3}$$

The vertical velocity component is obtained by differentiation of φ_P. Thus

$$w_P = \frac{\partial \varphi_P}{\partial z} = \int_{\sqrt{y^2+z^2}}^{x} \frac{\partial u}{\partial z} dx \tag{4}$$

since at the lower limit $u = 0$ in accordance with equation (1).

In considering point Q, it is convenient to evaluate equation (2) in several steps: first through the plane wave, then from the plane wave to the Mach cone, and finally from the Mach cone to the point Q. In passing through the tangent plane, the value of the term $\cos^{-1}(x'/\sqrt{y'^2+z'^2})$ in equation (1) jumps from 0 to π; thus, the discontinuity in u is finite, and there is no discontinuity in φ. Hence, the lower limit of the integrals may be taken as the value of x at the plane wave, $y/m + \frac{z\sqrt{m^2-1}}{m}$. Between the plane wave and the Mach cone the value of u is constant at $-V_o m\alpha/\sqrt{m^2-1}$ so that within this region the potential is

$$\varphi_{wc} = \int_{\frac{y}{m} + \frac{z\sqrt{m^2-1}}{m}}^{x} u dx = -\frac{V_o m\alpha}{\sqrt{m^2-1}}\left(x - \frac{y}{m} - \frac{z\sqrt{m^2-1}}{m}\right) \tag{5}$$

$$w_{wc} = \frac{\partial \varphi}{\partial z} = V_o \alpha \tag{6}$$

This equation shows that the vertical velocity is constant in the whole region between the plane wave and the Mach cone.

When the integration is carried from the Mach cone to point Q, it is noted from equation (5) that the potential at the Mach cone is

$$\varphi_c = -\frac{V_o m\alpha}{\sqrt{m^2-1}}\left(\sqrt{y^2+z^2} - \frac{y}{m} - z\frac{\sqrt{m^2-1}}{m}\right) \tag{7}$$

and therefore the potential at point Q is

$$\varphi_Q = -\frac{V_o m\alpha}{\sqrt{m^2-1}}\left(\sqrt{y^2+z^2} - \frac{y}{m} - \frac{z\sqrt{m^2-1}}{m}\right) + \int_{\sqrt{y^2+z^2}}^{x} u dx \tag{8}$$

Differentiating to obtain the vertical velocity

$$w_Q = V_0\alpha + \int_{\sqrt{y^2+z^2}}^{x} \frac{\partial u}{\partial z}\, dx \tag{9}$$

Equations (4) and (9) give the value of the vertical velocity at points P and Q. Although both equations contain the same integral, the actual value of the integral will depend on the path of integration. The integral is evaluated in Appendix A for each path; thus, for point P

$$\int_{\sqrt{y^2+z^2}}^{x} \frac{\partial u}{\partial z}\, dx = \frac{V_0\alpha}{\pi} \cos^{-1} \frac{yy'+z^2}{\sqrt{y^2+z^2}\,\sqrt{y'^2+z'^2}} \tag{10}$$

and for point Q

$$\int_{\sqrt{y^2+z^2}}^{x} \frac{\partial u}{\partial z}\, dx = \frac{V_0\alpha}{\pi} \cos^{-1}\left(\frac{yy'+z^2}{\sqrt{y^2+z^2}\,\sqrt{y'^2+z'^2}}\right) - V_0\alpha \tag{11}$$

If the values of the integral given by equations (10) and (11) are substituted into equations (4) and(9), respectively, identical results for the vertical velocities at points P and Q are obtained. Thus

$$w_P = w_Q = \frac{V_0\alpha}{\pi} \cos^{-1}\left(\frac{yy' + z^2}{\sqrt{y^2+z^2}\,\sqrt{y'^2+z'^2}}\right) \tag{12}$$

Equation (12) represents the vertical velocity due to one line-pressure source. The vertical velocity due to both pressure sources is obtained by adding to this result the contribution of the other pressure source which is determined by substituting $-y$ for y in equation (12). In accordance with previous considerations, the vertical velocity for the triangular lifting wing is of opposite sign to the vertical velocity due to the two pressure sources, thus

$$w = -\frac{V_0\alpha}{\pi}\left\{\cos^{-1}\left[\frac{y(y-mx)+z^2}{\sqrt{y^2+z^2}\,\sqrt{(y-mx)^2 - z^2\,(m^2-1)}}\right] + \cos^{-1}\left[\frac{y(y+mx)+z^2}{\sqrt{y^2+z^2}\,\sqrt{(y+mx)^2 - z^2\,(m^2-1)}}\right]\right\} \tag{13}$$

LIFTING TRIANGLE OF INFINITE CHORD WITH SUBSONIC LEADING EDGES

The lift of a flat triangular wing with leading edges swept behind the Mach cone has been treated theoretically by H. J. Stewart in reference 7. In that paper a differential equation is derived for the complex downwash function, the real part of which is the vertical velocity. To determine the vertical velocity w, it is necessary to integrate the differential equation and determine the real part of the solution.

In the notation of this paper, Stewart's differential equation is

$$\frac{dw}{d\zeta} = \frac{2V_0\alpha}{mE(\sqrt{1-m^2})} \frac{(1+\zeta)^2}{(\zeta^2+s_0^2)^{3/2}\left(\zeta^2+\frac{1}{s_0^2}\right)^{3/2}} \tag{14}$$

The actual integration of this equation is accomplished in Appendix B, from which it is found that

$$W = w+i\overline{w} = \frac{2V_0\alpha s_0}{mE(\sqrt{1-m^2})\ (1+s_0^2)^2}[(1+2s_0^2)\ F(\xi, \sqrt{1-s_0^4})$$

$$+ E(\xi, \sqrt{1-s_0^4}) + F(\eta, \sqrt{1-s_0^4}) - E(\eta, \sqrt{1-s_0^4})] + C \tag{15}$$

In this equation, the complex variables ξ and η are related to y/x and z/x by the following equations:

$$\zeta = \frac{(y/x) + i\ (z/x)}{1 + \sqrt{1-(y/x)^2 - (z/x)^2}} \tag{16}$$

$$\xi = \frac{\zeta}{\sqrt{\zeta^2+s_0^2}} \tag{17}$$

$$\eta = \frac{1}{\sqrt{1+s_0^2\zeta^2}} \tag{18}$$

The value of the constant C may be determined from the boundary condition that $w = -V_0\alpha$ on the wing.

The vertical velocity w is the real part of the downwash function W in equation (15). Thus, it is necessary to determine the real part of the elliptic integrals appearing in the equation. The methods used to obtain the real part of the incomplete elliptic integrals of the first and second kinds are described in Appendixes C and D, respectively. Using the results of these appendixes, the final expression for the vertical velocity is

$$w = \frac{2V_o\alpha s_o}{mE(\sqrt{1-m^2})\ (1+s_o^2)^2}\left\{(1+2s_o^2)\ F(\sqrt{\lambda_1}, \sqrt{1-s_o^4})\right.$$

$$+ E(\sqrt{\lambda_1}, \sqrt{1-s_o^4}) + \frac{(1-s_o^4)\cdot\sigma_1\sqrt{\lambda_1(1-\lambda_1)\ [1-(1-s_o^4)\lambda_1]}}{1-\sigma_1\ [1-(1-s_o^4)\lambda_1]}$$

$$+ F(\sqrt{\lambda_2}, \sqrt{1-s_o^4}) - E(\sqrt{\lambda_2}, \sqrt{1-s_o^4})$$

$$\left.- \frac{(1-s_o^4)\ \sigma_2\sqrt{\lambda_2\ (1-\lambda_2)\ [1-(1-s_o^4)\lambda_2]}}{1-\sigma_2\ [1-(1-s_o^4)\lambda_2]}\right\} \tag{19}$$

On the basis of conical flow considerations, the vertical velocity is constant along rays through the apex of the lifting triangle and thus depends only on y/x and z/x. In order to determine the vertical velocity for a ray defined by y/x and z/x, the real and imaginary parts of ξ and η must be determined in accordance with equations (16), (17), and (18). From τ_1 and δ_1, the real and imaginary parts of ξ, the values of σ_1 and λ_1 are obtained using equations (C12) and (C13). Similarly, values of σ_2 and λ_2 are calculated for the complex variable η using these same equations. The vertical velocity w for the ray defined by y/x and z/x is then determined from equation (19) using these values of σ_1, λ_1, σ_2, and λ_2.

RESULTS AND DISCUSSION

Downwash Charts

The equations presented in this report permit determination of the downwash at any point in the induced flow fields of lifting triangles of infinite chord. The equations have been used to determine downwash charts for a number of such surfaces. The range of leading-edge sweep angle used in the calculation is sufficient to include

all practical configurations, and the number of lifting surfaces for which the charts have been determined is sufficient to permit interpolation. The charts are presented in figures 3(a) to 3(h) and show lines of constant $d\epsilon/d\alpha$ within the Mach cone in a plane perpendicular to the flight direction. Since the downwash field is conical, the downwash pattern is similar in all planes perpendicular to the flight direction. Only one quadrant of the Mach cone is shown since the downwash pattern is symmetrical with respect to both the horizontal and vertical planes of symmetry.

In determining the charts for the various lifting triangles, the values of $d\epsilon/d\alpha$ were calculated at a number of points in the Mach cone for $M_o = \sqrt{2}$. The lines of constant $d\epsilon/d\alpha$ were then determined from cross plots. Although the calculations have been made for $M_o = \sqrt{2}$, in which case $d\epsilon/d\alpha$ depends only on m, y/x, and z/x, it can be shown by the Glauert-Prandtl rule that $d\epsilon/d\alpha$ for any Mach number depends only on $m\sqrt{M_o^2-1}$, $(y\sqrt{M_o^2-1})/x$, and $(z\sqrt{M_o^2-1})/x$. These parameters have been utilized in the charts of figure 3 so that the results are applicable at Mach numbers other than $\sqrt{2}$.

In determining the value of $d\epsilon/d\alpha$ at any point in the field for a given finite swept wing, the value of $d\epsilon/d\alpha$ for the corresponding lifting triangle of infinite chord is first determined from figure 3. If the point in question is not within the region influenced by the trailing edge or the tips, this value will represent the total $d\epsilon/d\alpha$. However, if the point lies within the region of influence of the trailing edge or tips, the value determined from figure 3 represents only part of the actual value of $d\epsilon/d\alpha$. For a finite lifting triangle, the remaining part, which consists of the contribution to the downwash of the trailing edge, can be determined by the method of Lagerstrom (reference 4). In the more general case of a finite swept wing, it is necessary to take account of the sweep angle of the trailing edge and the effect of the tips by a similar method of lift cancellation.

Variation of Downwash Distribution With Leading-Edge Sweep Angle

The plots of figure 3 show the changes in the downwash distribution as the sweep angle of the leading edge is increased with respect to the Mach cone. When the leading edge of the wing is considerably ahead of the Mach cone (large values of $m\sqrt{M_o^2-1}$), $d\epsilon/d\alpha$ is large throughout the Mach cone and the rate of change of $d\epsilon/d\alpha$ with distance above or below the chord plane is small for considerable distances from

the chord plane. Between the Mach cone and the plane waves from the leading edges, which are tangent to the Mach cone, the value of $d\epsilon/d\alpha$ is constant and equal to unity. The surfaces of constant downwash intersect at the lines of tangency of the plane waves and the Mach cone. As the sweep of the leading edge is increased ($m\sqrt{M_o^2-1}$ decreases), the line of tangency moves along the Mach cone toward the chord plane and the rate of change of $d\epsilon/d\alpha$ with distance from the chord plane increases. When $m\sqrt{M_o^2-1}$ approaches 1, the lines of tangency and the leading edge approach coincidence on the Mach cone; and when $m\sqrt{M_o^2-1}$ is equal to 1, the surfaces of constant downwash intersect on this line of coincidence.

When the leading edge becomes subsonic, there are two qualitative changes in the downwash pattern. First, the surfaces of constant downwash intersect at the leading edges rather than at the lines of tangency, which no longer exist; second, a region of upwash occurs between the Mach cone and the leading edge. This region of upwash increases in extent as the sweep of the leading edge increases. In addition, the rate of change of $d\epsilon/d\alpha$ with distance above or below the lifting surface increases rapidly, and the downwash near the surface of the Mach cone becomes very small. In the limit, as the direction of the leading edge coincides with the free-stream direction, the downwash field disappears.

Additional Factors Affecting the Downwash

When the charts of this report are used in conjunction with the lift-cancellation method to obtain the downwash behind finite swept wings, certain factors which have not been discussed thus far must be considered. In the linearized theory of supersonic flow the assumption is made that the trailing vortex sheet is coincident with the extended chord plane. This assumption, although valid for very small angles of attack, will probably cause an appreciable error at large angles of attack for which the trailing vortex sheet is displaced from the extended chord plane due to the action of the downwash. An additional effect, which is important in the immediate vicinity of the wake boundaries, is inflow to the wake resulting from the viscous properties of the fluid. The influence on the downwash at subsonic speeds of these two factors has been investigated and methods for predicting their influence have been reported in reference 1. However, sufficient experimental data are not yet available to permit the development of similar methods for supersonic flow.

Another factor that is neglected by the linear theory is the

curling up of the vortex sheet behind the wing tips. This effect is neglected in subsonic flow calculations for conventional high-aspect-ratio wings. However, for the low-aspect-ratio wings which will probably be used with some types of supersonic aircraft, this effect may be important.

Ames Aeronautical Laboratory,
National Advisory Committee for Aeronautics,
Moffett Field, Calif.

APPENDIX A

EVALUATION OF INTEGRAL IN EQUATIONS (4) AND (9)

The integral to be evaluated is

$$I = \int_{\sqrt{y^2+z^2}}^{x} \left(\frac{\partial u}{\partial z}\right) dx \tag{A1}$$

in which

$$u = -\,\mathrm{r.p.}\ \frac{V_0\alpha}{\pi} \frac{m}{\sqrt{m^2-1}} \cos^{-1}\left(\frac{x'}{\sqrt{y'^2+z'^2}}\right) \tag{A2}$$

The value of $\partial u/\partial z$ is determined from equation (A2) and substituted into equation (A1), with the quantities x', y', and z' replaced by $x-my$, $y-mx$, and $z\sqrt{1-m^2}$, respectively. Thus

$$I = \frac{V_0\alpha}{\pi} mz \int_{\sqrt{y^2+z^2}}^{x} \frac{(x-my)\,dx}{\left[(y-mx)^2-z^2(m^2-1)\right]\sqrt{x^2-y^2-z^2}} \tag{A3}$$

From the identity

$$\frac{x-my}{(y-mx)^2-z^2(m^2-1)} \equiv \frac{1}{2mz\sqrt{m^2-1}} \left[\frac{y(m^2-1)-z\sqrt{m^2-1}}{y+z\sqrt{m^2-1}-mx} - \frac{y(m^2-1)+z\sqrt{m^2-1}}{y-z\sqrt{m^2-1}-mx}\right] \tag{A4}$$

the integration can be accomplished by separating the integral into two parts. Thus

$$I = \frac{V_o\alpha}{2\pi}\left\{\tan^{-1}\left[\frac{m(y^2+z^2)-x(y+z\sqrt{m^2-1})}{(y\sqrt{m^2-1}-z)\ \sqrt{x^2-y^2-z^2}}\right]\right.$$

$$\left.-\tan^{-1}\left[\frac{m(y^2+z^2)-x(y-z\sqrt{m^2-1})}{(y\sqrt{m^2-1}+z)\ \sqrt{x^2-y^2-z^2}}\right]\right\}_{\sqrt{y^2+z^2}}^{x} \tag{A5}$$

Before substituting the limits, it is convenient to replace the inverse-tangent difference by the equivalent inverse cosine.

$$I = \frac{V_o\alpha}{\pi}\left\{\cos^{-1}\left[\frac{y(y-mx)+z^2}{\sqrt{y^2+z^2}\ \sqrt{(y-mx)^2-z^2(m^2-1)}}\right]\right\}_{\sqrt{y^2+z^2}}^{x} \tag{A6}$$

In this equation the positive roots of the radicals are to be used together with the principal values of the inverse cosine. At the lower limit where

$$x^2 = y^2+z^2$$

and

$$(x-my)^2 = (y-mx)^2 - z^2(m^2-1)$$

the principal value of the inverse cosine is zero for $y<x/m$ and π for $y>x/m$. It can be shown from figure 2 that $y<x/m$ corresponds to point P and $y>x/m$ corresponds to point Q.

Therefore, for point P

$$\int_{\sqrt{y^2+z^2}}^{x} \frac{\partial u}{\partial z}\,dx = \frac{V_o\alpha}{\pi}\cos^{-1}\left(\frac{yy'+z^2}{\sqrt{y^2+z^2}\ \sqrt{y'^2+z'^2}}\right) \tag{A7}$$

and for point Q

$$\int_{\sqrt{y^2+z^2}}^{x} \frac{\partial u}{\partial z}\,dx = \frac{V_o\alpha}{\pi}\left[\cos^{-1}\left(\frac{yy'+z^2}{\sqrt{y^2+z^2}\ \sqrt{y'^2+z'^2}}\right)-\pi\right] \tag{A8}$$

APPENDIX B

INTEGRATION OF STEWART'S DIFFERENTIAL EQUATION

In determining W from Stewart's differential equation

$$\frac{dW}{d\zeta} = \frac{2V_0\alpha}{mE(\sqrt{1-m^2})} \frac{(1+\zeta^2)^2}{(\zeta^2+s_0^2)^{3/2}\left(\zeta^2+\frac{1}{s_0^2}\right)^{3/2}} \tag{B1}$$

it is convenient to express the downwash function as the sum of three integrals

$$W = \frac{2V_0\alpha\, s_0^3}{mE(\sqrt{1-m^2})(1-s_0^4)}\left[\frac{1-s_0^4}{s_0^2}\int\frac{d\zeta}{\sqrt{\zeta^2+s_0^2}\,\sqrt{\zeta^2 s_0^2+1}}\right.$$

$$\left.+(1-s_0^2)^2\int\frac{d\zeta}{(\zeta^2+s_0^2)^{3/2}\sqrt{\zeta^2 s_0^2+1}} - \frac{(1-s_0^2)^2}{s_0^2}\int\frac{d\zeta}{(\zeta^2 s_0^2+1)^{3/2}\sqrt{\zeta^2+s_0^2}}\right] \tag{B2}$$

Introducing the change of independent variable

$$\xi = \frac{\zeta}{\sqrt{\zeta^2+s_0^2}} \tag{B3}$$

the first two integrals become

$$\int\frac{d\zeta}{\sqrt{\zeta^2+s_0^2}\,\sqrt{\zeta^2 s_0^2+1}} = F(\xi, \sqrt{1-s_0^4}) \tag{B4}$$

$$\int\frac{d\zeta}{(\zeta^2+s_0^2)^{3/2}\sqrt{\zeta^2 s_0^2+1}} = \frac{1}{s_0^2}\frac{\sqrt{1-\xi^2}}{\sqrt{1-(1-s_0^2)\xi^2}}$$

$$= -\frac{s_0^2}{(1-s_0^4)}F(\xi, \sqrt{1-s_0^4}) + \frac{1}{s_0^2(1-s_0^4)}E(\xi, \sqrt{1-s_0^4}) \tag{B5}$$

Making use of the transformation

$$\eta = \frac{1}{\sqrt{1+s_0^2\zeta^2}} \tag{B6}$$

the third integral becomes

$$\int \frac{d\zeta}{(\zeta^2 s_o^2 + 1)^{3/2}\sqrt{\zeta^2 + s_o^2}} = -\int \frac{\eta^2 d\eta}{\sqrt{1-\eta^2}\sqrt{1-\eta^2(1-s_o^4)}}$$

$$= \frac{1}{(1-s_o^4)}\left[E(\eta,\sqrt{1-s_o^4}) - F(\eta,\sqrt{1-s_o^4})\right] \tag{B7}$$

Substituting these results into equation (B2) the equation for the downwash function becomes

$$W = w+i\overline{w} = \frac{2V_o\alpha s_o}{mE(\sqrt{1-m^2})\ (1+s_o^2)^2}\left[(1+2s_o^2)\ F(\xi,\sqrt{1-s_o^4})\right.$$

$$\left. + E(\xi,\sqrt{1-s_o^4}) + F(\eta,\sqrt{1-s_o^4}) - E(\eta,\sqrt{1-s_o^4})\right] + C \tag{B8}$$

The constant C is to be chosen so that w, the real part of W, is zero on the Mach cone.

APPENDIX C

DETERMINATION OF THE REAL PART OF THE INCOMPLETE ELLIPTIC INTEGRAL OF THE FIRST KIND

The Jacobian normal form of the incomplete elliptic integral of the first kind in the complex plane is determined as follows:

$$F(\tau + i\delta,k) \equiv \int_0^{\tau+i\delta} \frac{d\xi}{\sqrt{1-\xi^2}\sqrt{1-k^2\xi^2}}\ . \tag{C1}$$

In determining the real and imaginary parts F_r and F_i of this integral, it is convenient to introduce the Jacobian sine amplitude elliptic function,

$$\mathrm{sn}\ (F_r + iF_i,k) = \tau + i\delta \tag{C2}$$

Making use of the addition formula for the sine amplitude function

$$sn(F_r+iF_i,k) = \frac{sn(F_r,k)cn(iF_i,k)dn(iF_i,k)+sn(iF_i,k)cn(F_r,k)dn(F_r,k)}{1-k^2sn^2(F_r,k)sn^2(iF_i,k)} \tag{C3}$$

Substituting the following relationships

$$\left.\begin{aligned} sn(iF_i,k) &= \frac{i\ sn(F_i,k')}{cn(F_i,k')} \\ cn(iF_i,k) &= \frac{1}{cn(F_i,k')} \\ dn(iF_i,k) &= \frac{dn(F_i,k')}{cn(F_i,k')} \end{aligned}\right\} \tag{C4}$$

equation (C3) becomes

$$sn(F_r+iF_i,k) = \frac{sn(F_r,k)dn(F_i,k')+i\ sn(F_i,k')cn(F_i,k')cn(F_r,k)dn(F_r,k)}{cn^2(F_i,k')+k^2sn^2(F_r,k)sn^2(F_i,k')} \tag{C5}$$

Separating equation (C5) into its real and imaginary parts

$$\tau = \frac{sn(F_r,k)dn(F_i,k')}{cn^2(F_i,k')+k^2sn^2(F_r,k)sn^2(F_i,k')} \tag{C6}$$

$$\delta = \frac{sn(F_i,k')cn(F_i,k')cn(F_r,k)dn(F_r,k)}{cn^2(F_i,k')+k^2sn^2(F_r,k)sn^2(F_i,k')} \tag{C7}$$

Introducing the substitutions

$$\lambda = sn^2(F_r,k) \tag{C8}$$

$$\sigma = sn^2(F_i,k') \tag{C9}$$

and making use of the identities

$$\mathrm{cn}(F_r,k) = \sqrt{1-\lambda}$$

$$\mathrm{dn}(F_r,k) = \sqrt{1-k^2\lambda}$$

$$\mathrm{cn}(F_i,k') = \sqrt{1-\sigma}$$

$$\mathrm{dn}(F_i,k') = \sqrt{1-k'^2\sigma}$$

equations (C6) and (C7) become

$$\tau^2 = \frac{\lambda(1-k'^2\sigma)}{(1-\sigma+k^2\lambda\sigma)^2} \tag{C10}$$

$$\delta^2 = \frac{\sigma(1-\sigma)\ (1-\lambda)\ (1-k^2\lambda)}{(1-\sigma+k^2\lambda\sigma)^2} \tag{C11}$$

Simultaneous solution of these equations yields

$$\lambda = \frac{\left[(1+\tau^2+\delta^2) - \sqrt{(1+\tau^2+\delta^2)^2 - 4\tau^2}\right]\left\{1+k^2(\tau^2+\delta^2) - \sqrt{\left[1+k^2(\tau^2+\delta^2)\right]^2 - 4k^2\tau^2}\right\}}{4k^2\tau^2} \tag{C12}$$

$$\sigma = \frac{(\tau^2+\delta^2-\lambda)}{(\tau^2+\delta^2-\lambda) - [\lambda k^2(\tau^2+\delta^2) - 1]} \tag{C13}$$

Therefore, to find the real and imaginary parts F_r and F_i, of the incomplete elliptic integral of which the sine amplitude is $\tau+i\delta$, it is first necessary to determine λ and σ from equations (C12) and (C13). Then from equations (C8) and (C9), it follows that

$$F_r = F(\sqrt{\lambda},k) \tag{C14}$$

$$F_i = F(\sqrt{\sigma},k') \tag{C15}$$

APPENDIX D

DETERMINATION OF THE REAL PART OF THE INCOMPLETE ELLIPTIC INTEGRAL OF THE SECOND KIND

The Jacobian normal form of the incomplete elliptic integral of the second kind in the complex plane is given as follows:

$$E(\tau+i\delta,k) \equiv \int_0^{\tau+i\delta} \frac{\sqrt{1-k^2\xi^2}}{\sqrt{1-\xi^2}}\, d\xi \tag{D1}$$

In determining the real and imaginary parts E_r and E_i of this integral, it is convenient to introduce the transformation

$$\xi = \mathrm{sn}(\mu,k) = \mathrm{sn}(\mu_r+i\mu_i,k) \tag{D2}$$

where the real and imaginary parts of μ are μ_r and μ_i, respectively. With this transformation equation (D1) becomes

$$E(\tau+i\delta,k) = \int_0^{F_r+iF_i} \mathrm{dn}^2(\mu,k)d\mu \tag{D3}$$

where the upper limit

$$F_r+iF_i = \int_0^{\tau+i\delta} \frac{d\xi}{\sqrt{1-\xi^2}\sqrt{1-k^2\xi^2}} \tag{D4}$$

is evaluated in accordance with the methods of Appendix C.

In integrating equation (D3) it is convenient to perform the integration in two steps. The first integration is along the real axis to F_r, and the second integration is along a line parallel to the imaginary axis from $\mu = F_r$ to $\mu = F_r+iF_i$. Thus equation (D3) becomes

$$E(\tau+i\delta,k) = \int_0^{F_r} \mathrm{dn}^2(\mu_r,k)d\mu_r + i\int_0^{F_i} \mathrm{dn}^2(F_r+i\mu_i,k)d\mu_i \tag{D5}$$

In determining the real part E_r of $E(\tau+i\delta,k)$ from equation (D5), it is noted that the first integral is real and is equal to $E(snF_r,k)$.

The determination of the real part of the second integral of equation (D5) may be performed with the help of the addition formula for the delta amplitude elliptic function

$$dn(F_r+i\mu_i,k) = \frac{dn(F_r,k)dn(i\mu_i,k) - k^2sn(F_r,k)sn(iF_i,k)cn(F_r,k)cn(iF_i,k)}{1-k^2sn^2(F_r,k)sn^2(iF_i,k)} \tag{D6}$$

Using the relationships for $sn(iF_i,k)$, $cn(iF_i,k)$ and $dn(iF_i,k)$ (See Appendix C.) in this equation, and substituting the imaginary part of the resulting expression for $dn(F_r+iF_i,k)$ into the second integral yields

$$\text{r.p. } i\int_0^{F_i} dn^2(F_r+i\mu_i,k)d\mu_i = 2k^2sn(F_r,k)cn(F_r,k)dn(F_r,k)\int_0^{F_i} \frac{cn(\mu_i,k')dn(\mu_i,k')sn(\mu_i,k')}{[cn^2(\mu_i,k')+k^2sn^2(F_r,k)sn^2(\mu_i,k')]^2}\,d\mu_i \tag{D7}$$

By direct integration of this equation

$$\text{r.p. } i\int_0^{F_i} dn^2(F_r+i\mu_i,k)d\mu_i = k^2sn(F_r,k)cn(F_r,k)dn(F_r,k)\,\frac{sn^2(F_i,k')}{1-sn^2(F_i,k')dn^2(F_r,k)} \tag{D8}$$

Combining the results for the first and second integrals

$$E_r = E(snF_r,k) + \frac{k^2sn(F_r,k)cn(F_r,k)dn(F_r,k)sn^2(F_i,k')}{1-sn^2(F_i,k')dn^2(F_r,k)} \tag{D9}$$

With the substitution of equations (C8) and (C9) of Appendix C, equation (D9) becomes

$$E_r = E(\sqrt{\lambda},k) + \frac{k^2\sqrt{\lambda}\sqrt{1-\lambda}\sqrt{1-k^2\lambda}\,\sigma}{1-\sigma(1-k^2\lambda)} \tag{D10}$$

Thus the real part of the incomplete elliptic integral of the second kind of sine amplitude $\tau+i\delta$ is obtained by evaluating λ and σ from equations (C12) and (C13) and substituting these values into equation (D10).

REFERENCES

1. Silverstein, Abe, Katzoff, S., and Bullivant, W. Kenneth: Downwash and Wake Behind Plain and Flapped Airfoils. NACA Rep. No. 651, 1939.

2. Nielsen, Jack N., and Sweberg, Harold H.: Note on Compressibility Effects on Downwash at the Tail at Subcritical Speeds. NACA CB No. L5C09, 1945.

3. Busemann, Adolf: Infinitesimal Conical Supersonic Flow. NACA TM No. 1100, 1947.

4. Lagerstrom, P.A., and Graham, Martha E.: Downwash and Sidewash Induced by Three-Dimensional Lifting Wings in Supersonic Flow. Douglas Aircraft Rep. No. SM-13007, Apr. 1947.

5. Heaslet, Max. A., and Lomax, Harvard: The Calculation of Downwash Behind Supersonic Wings With an Application to Triangular Plan Forms. NACA TN No. 1620, 1948.

6. Jones, Robert T.: Thin Oblique Airfoils at Supersonic Speed. NACA TN No. 1107, 1946.

7. Stewart, H. J.: The Lift of a Delta Wing at Supersonic Speeds. Quart. App. Math., vol. 4, no. 3, Oct. 1946, pp. 246-254.

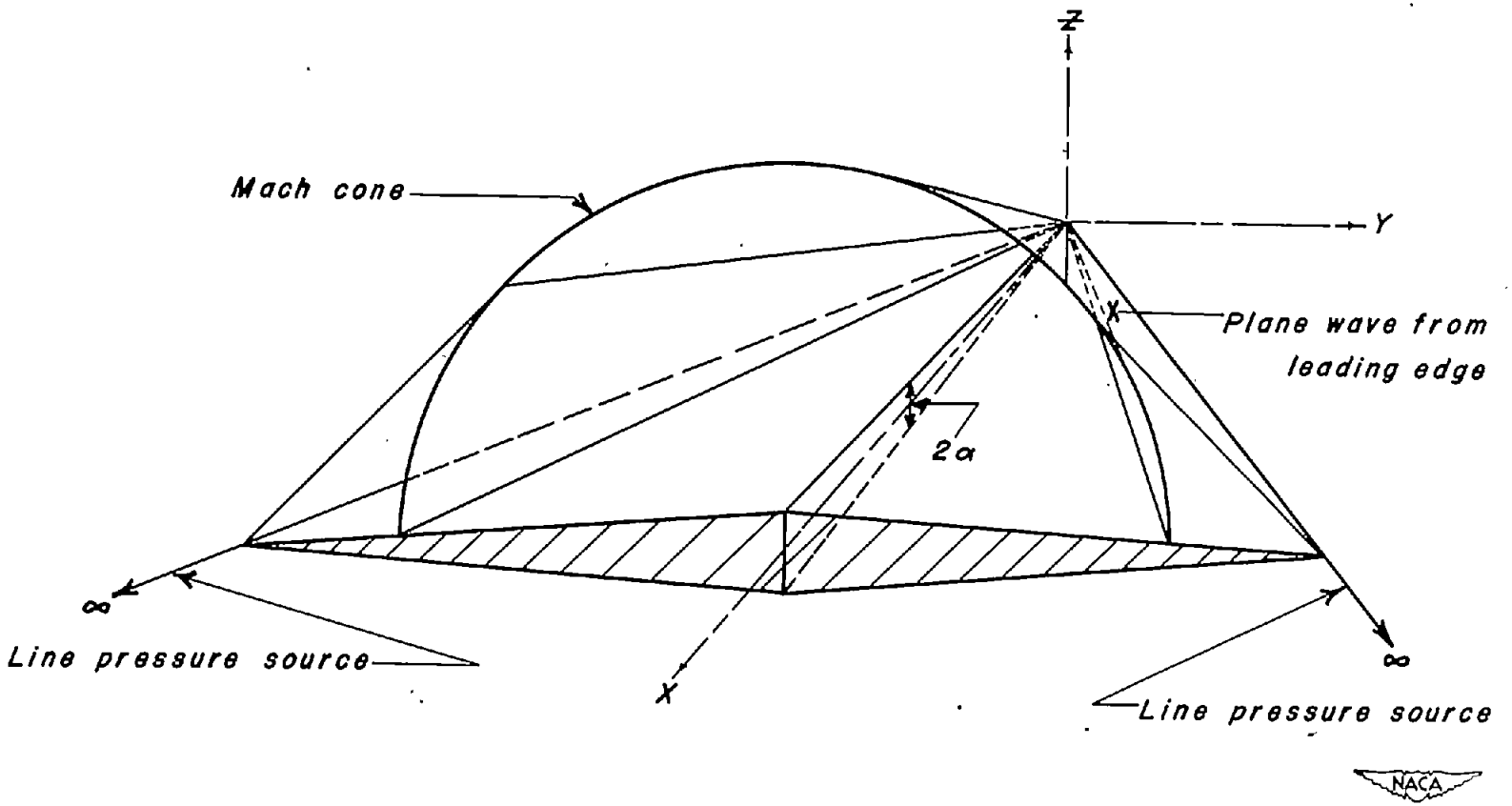

Figure 1.—Wing and Mach wave system

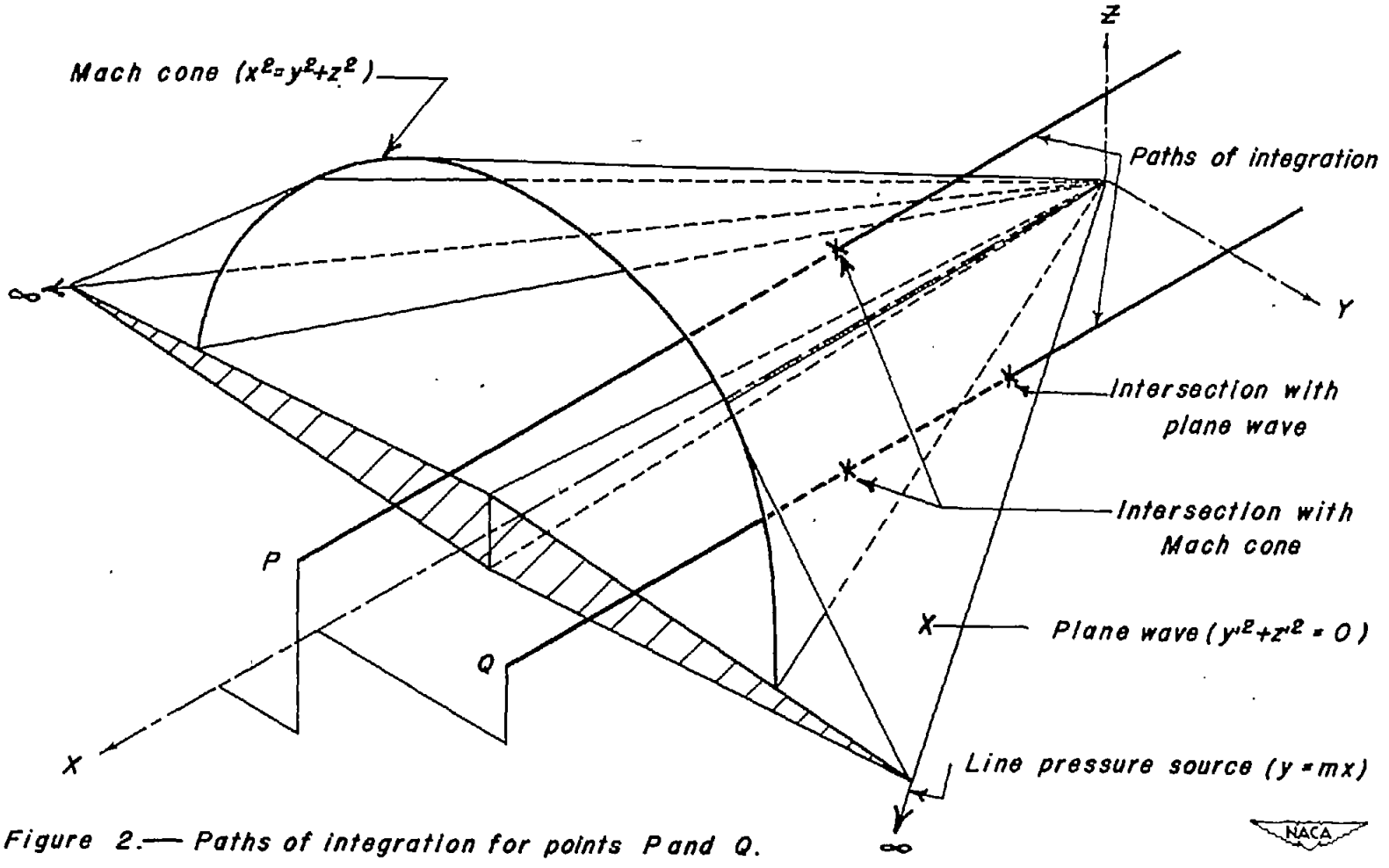

Figure 2.— Paths of integration for points P and Q.

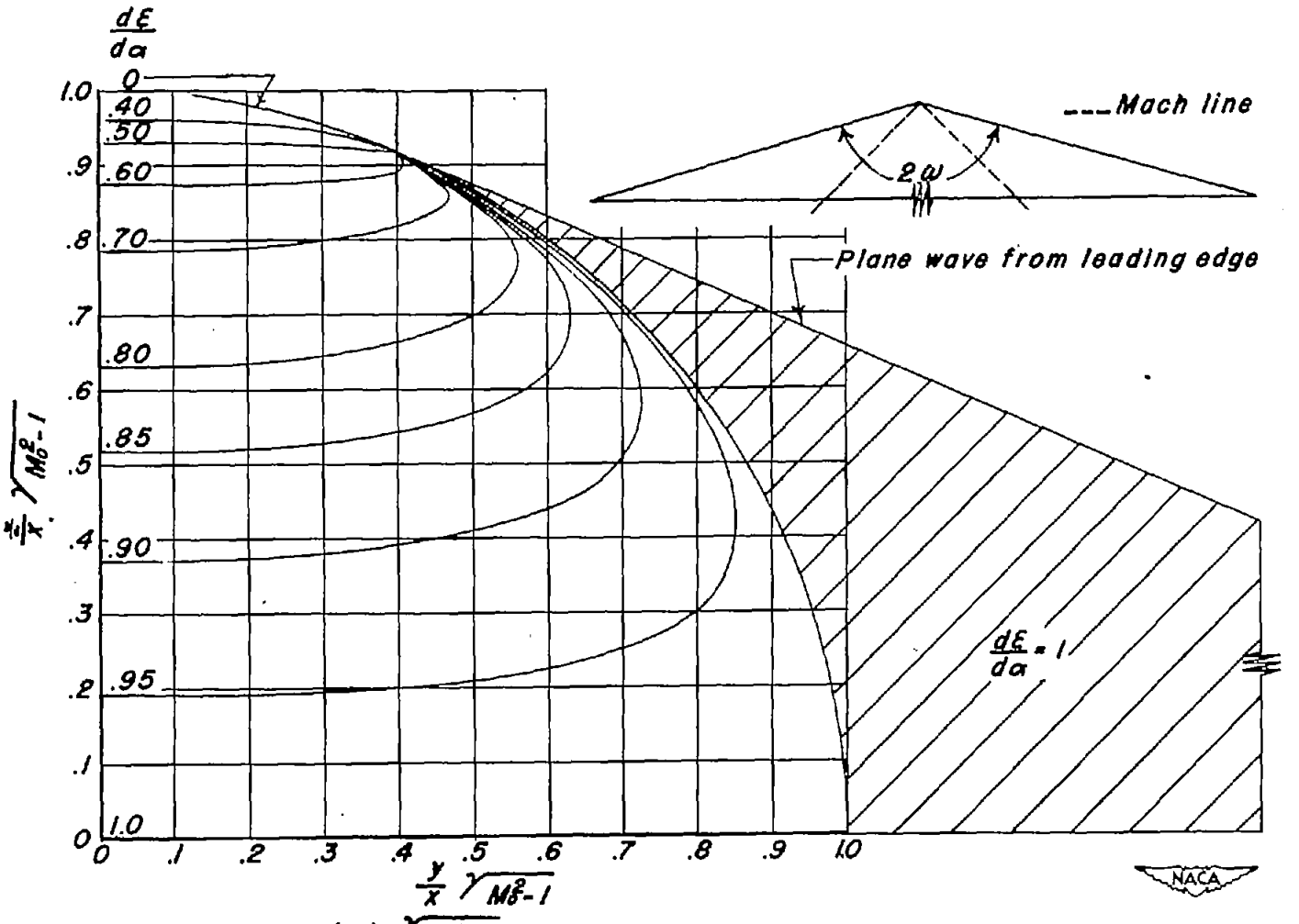

(a) $\sqrt{M_0^2-1}\tan\omega = 2.5$

Figure 3.— Downwash contours for lifting triangles of infinite chord.

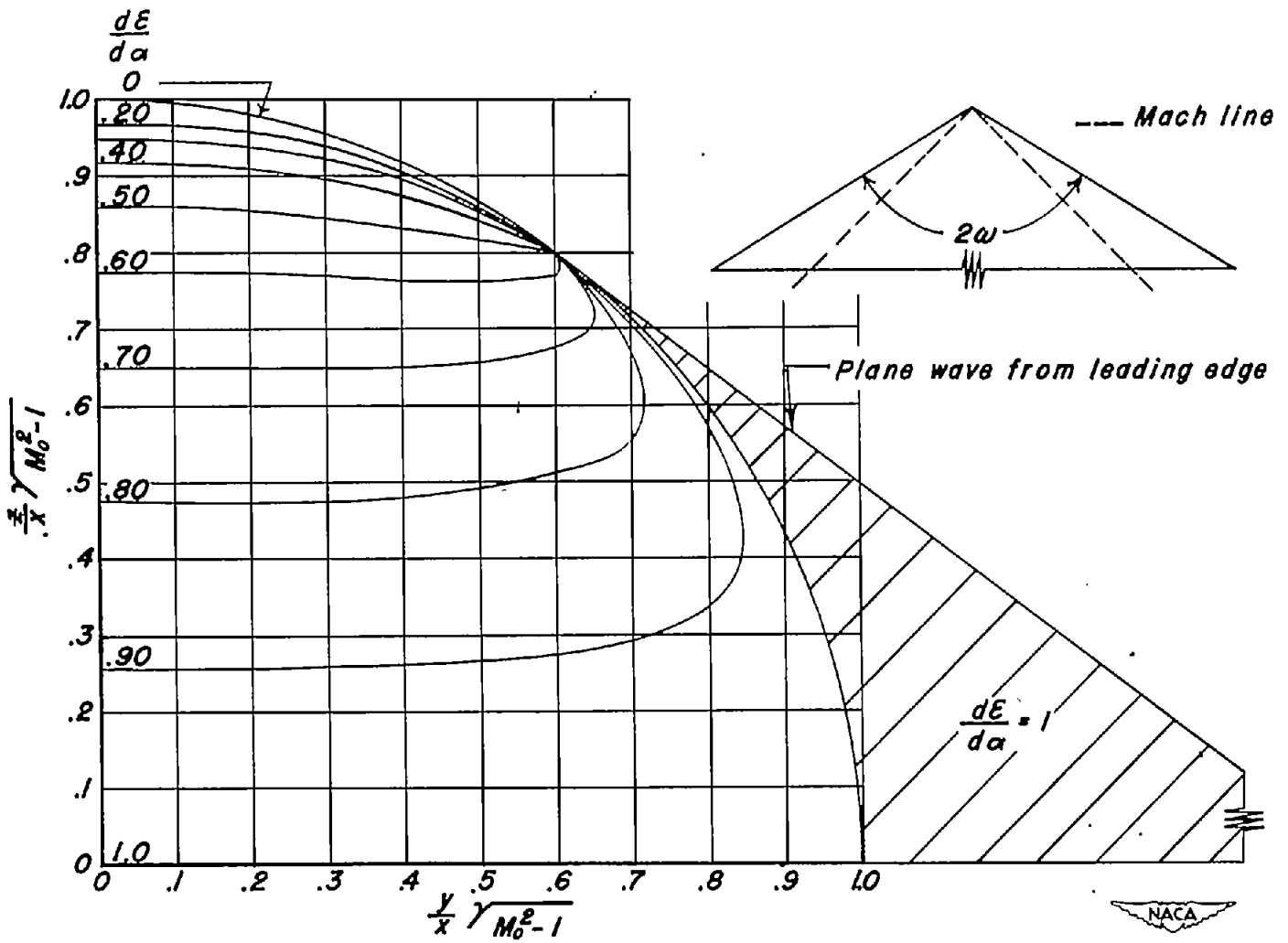

(b) $\sqrt{M_0^2-1}\tan\omega = 1.667$

Figure 3.— Continued

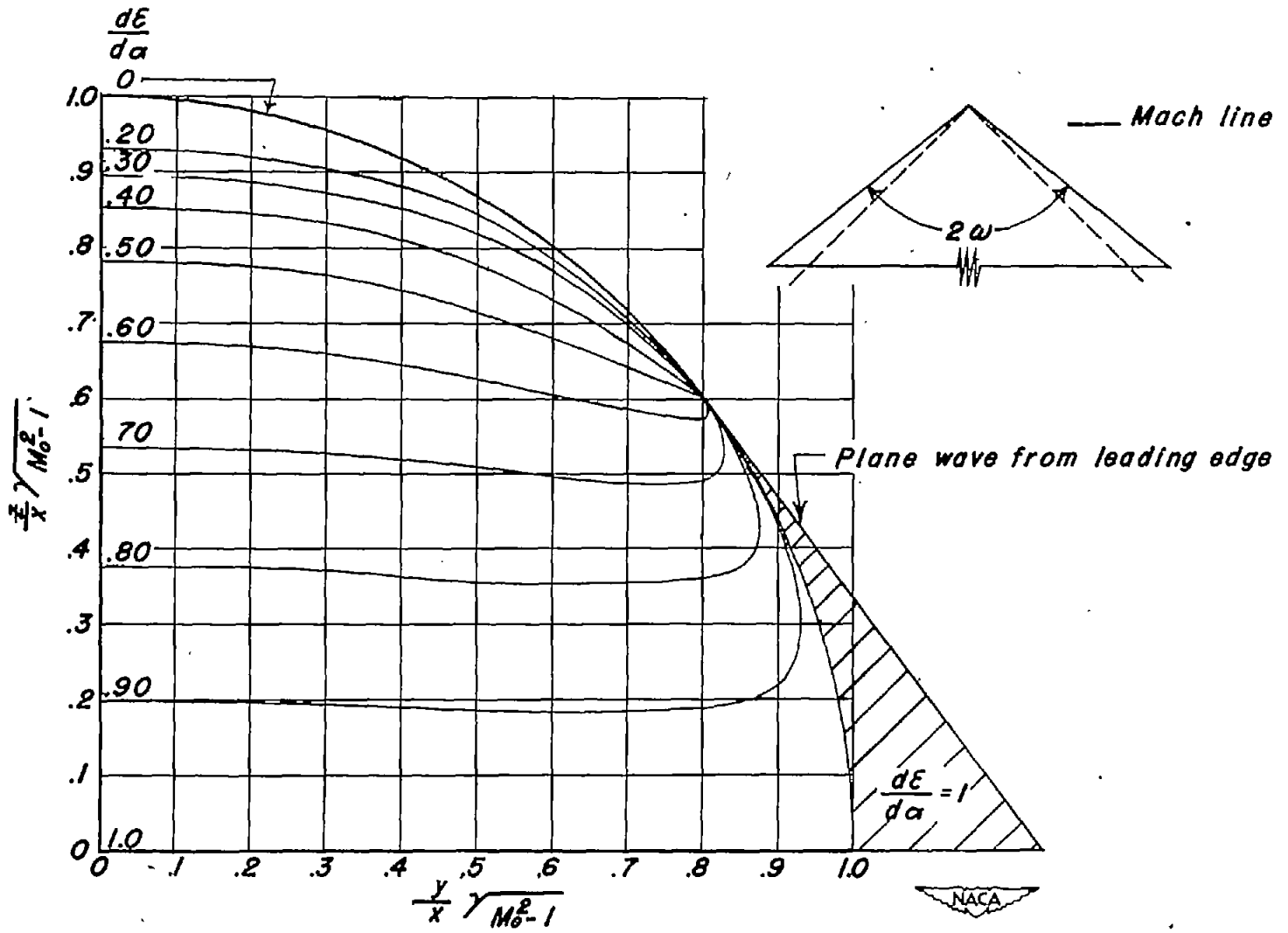

(c) $\sqrt{M_0^2-1}\tan\omega = 1.25$

Figure 3.— Continued

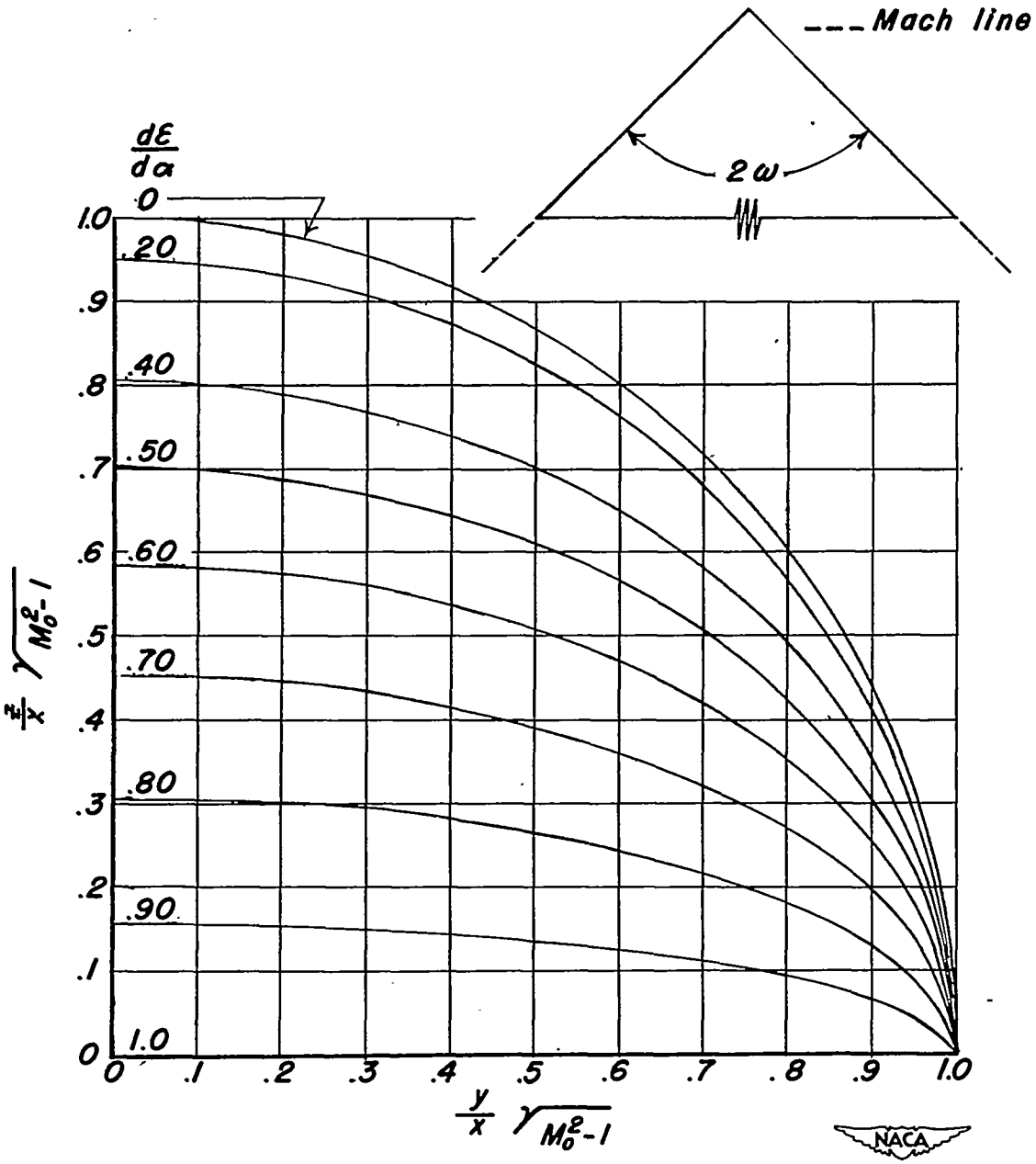

(d) $\sqrt{M_0^2-1}\tan\omega = 1.0$

Figure 3.— Continued

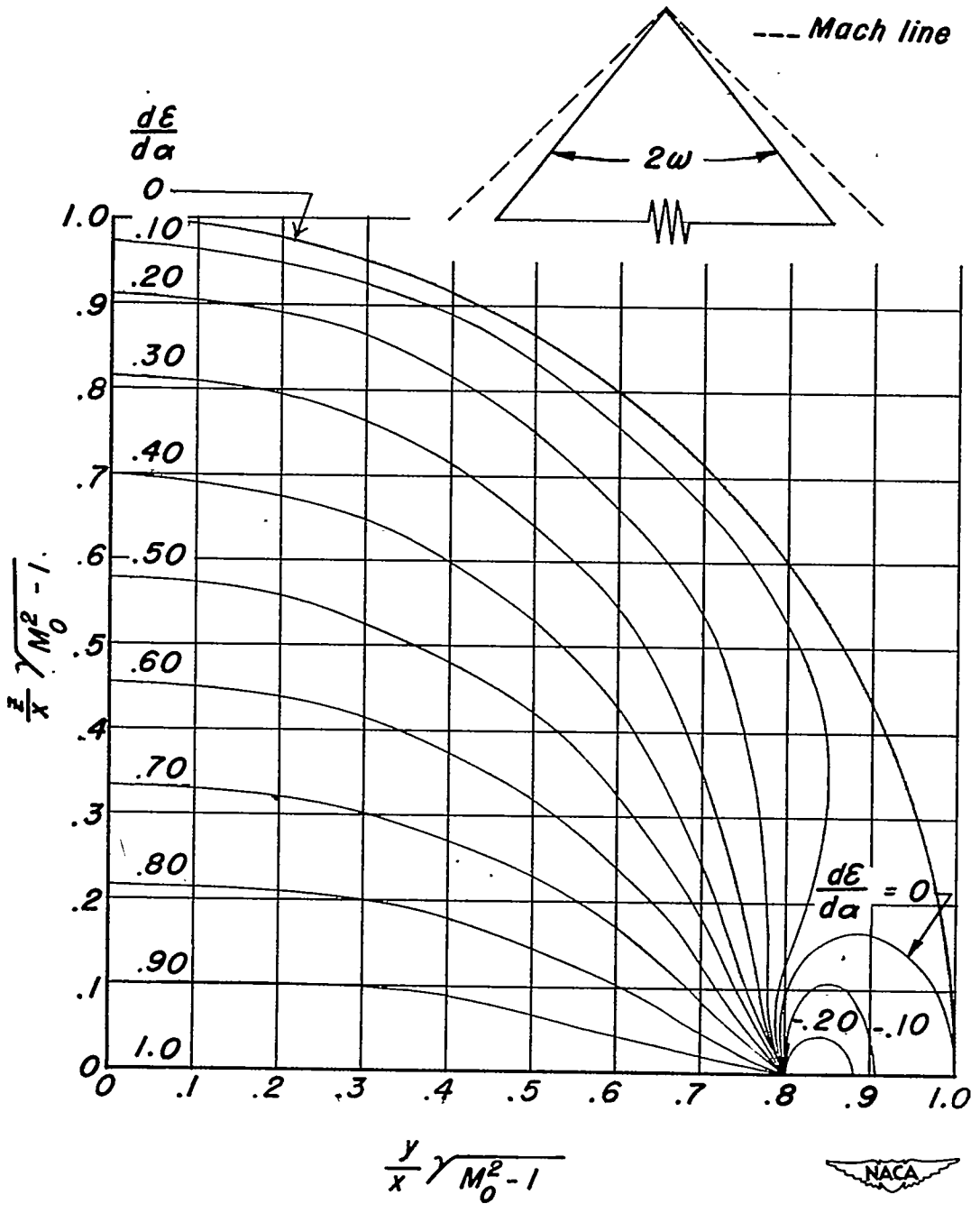

(e) $\sqrt{M_0^2-1}\ \tan\omega = .8$

Figure 3.— Continued

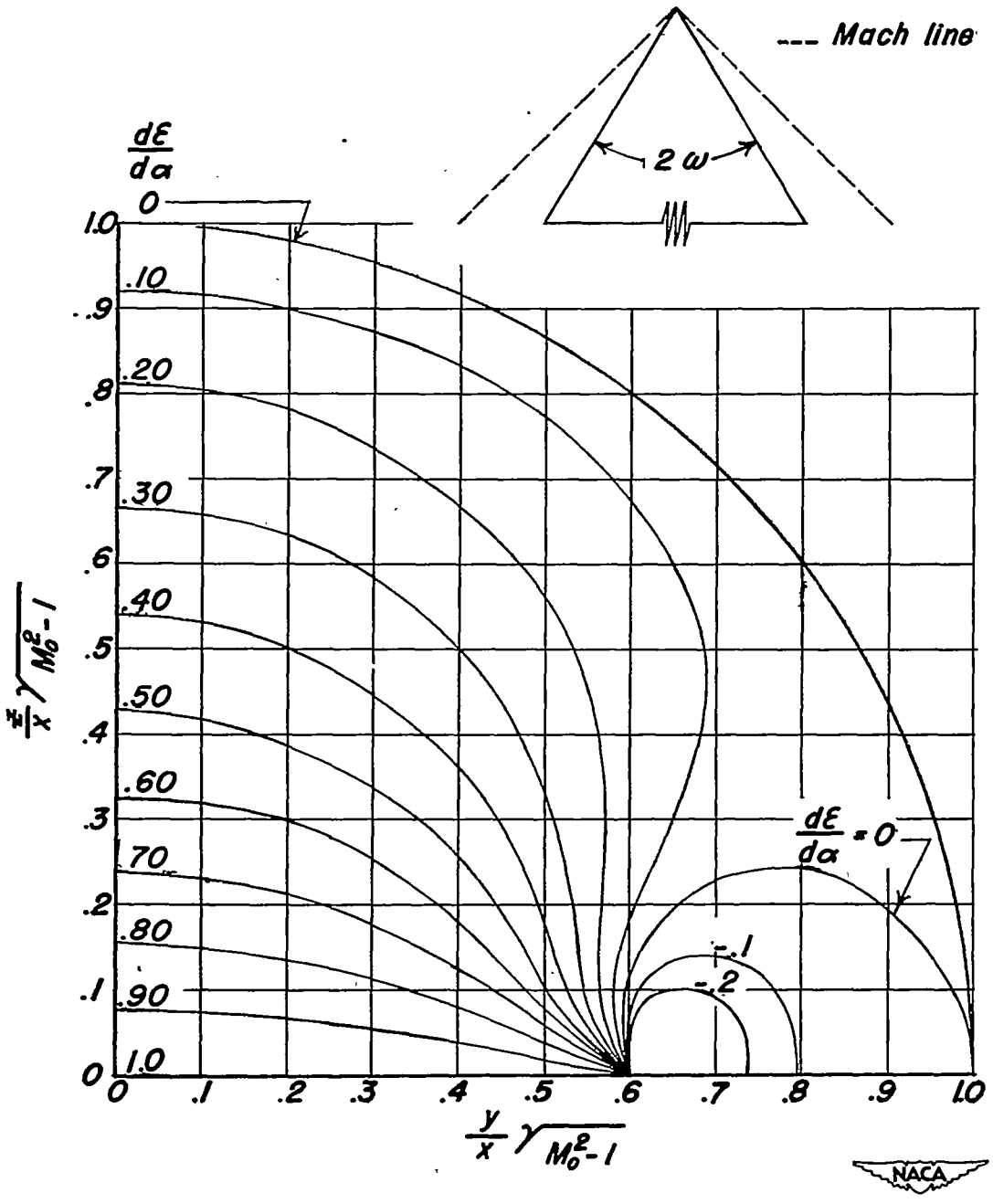

(f) $\sqrt{M_0^2-1}\tan\omega = .6$

Figure 3.—Continued

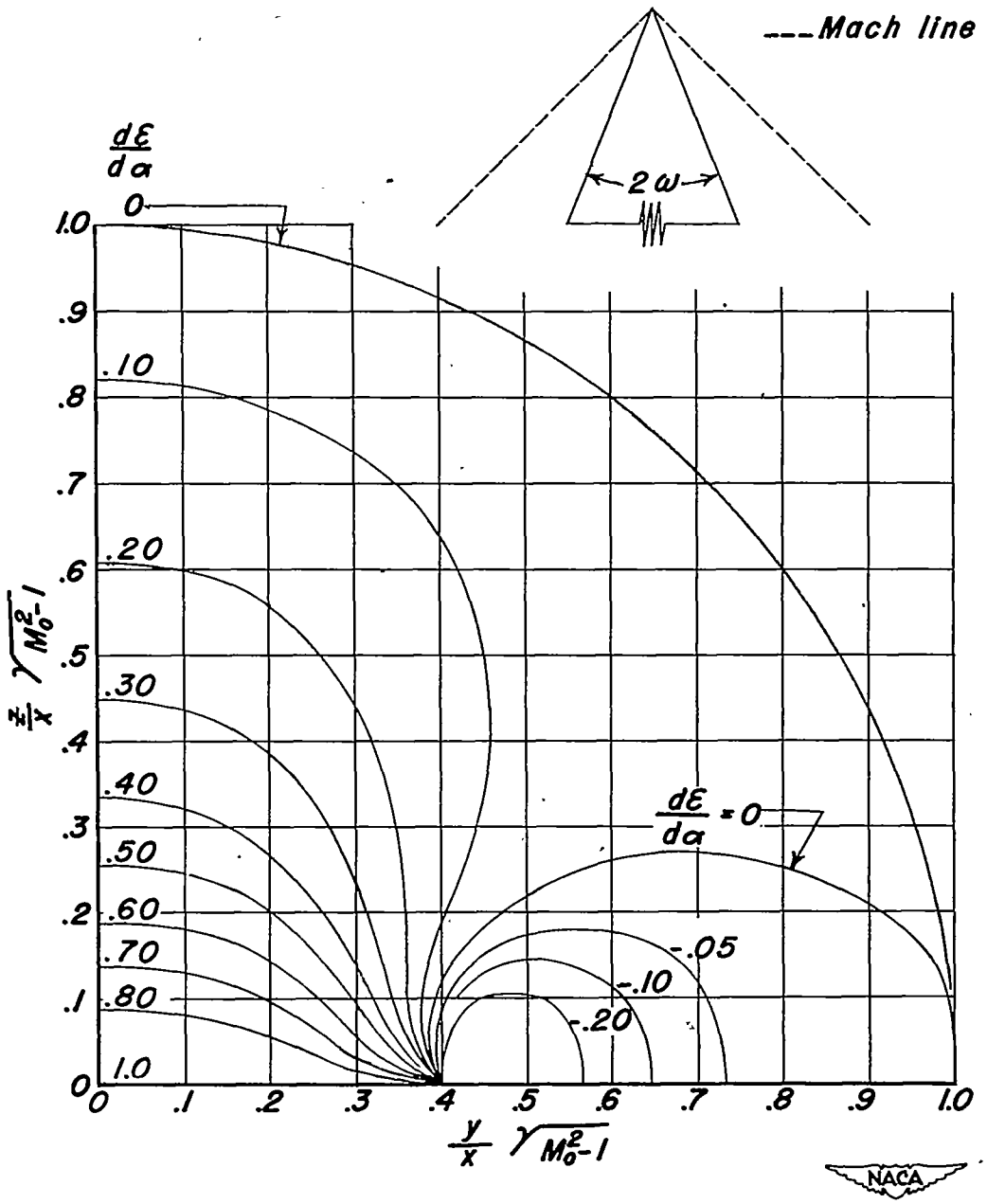

(g) $\sqrt{M_0^2 - 1} \tan \omega = .4$

Figure 3.—Continued

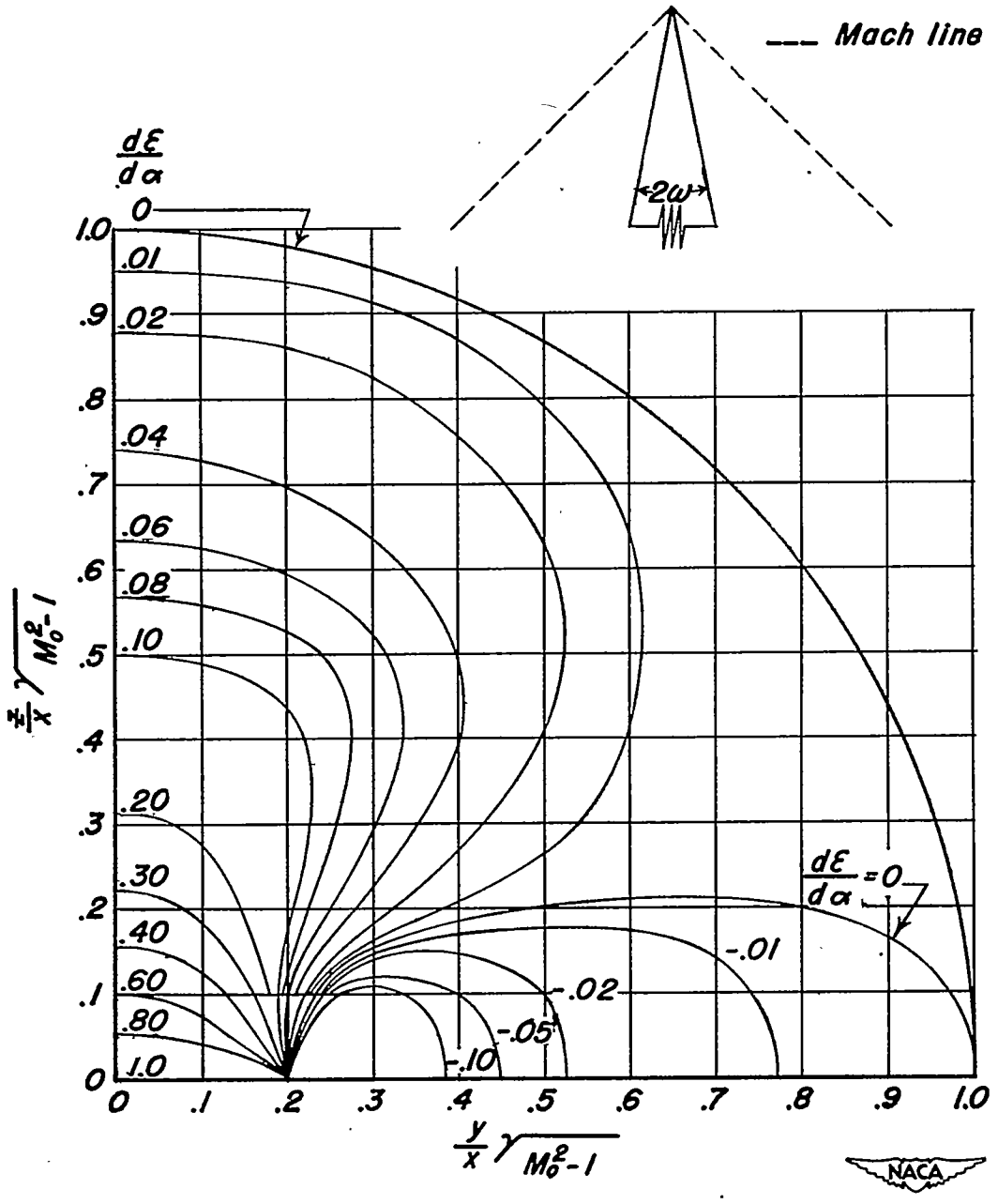

(h) $\sqrt{M_0^2 - 1}\tan\omega = .2$

Figure 3.— Concluded